An unusual O 2– /F – distribution in the new pyrochlore oxyfluorides: Na 2 B 2 O 5 F 2 (B = Nb, Ta)

Edouard Boivin, Frédérique Pourpoint, Sébastien Saitzek, Pardis Simon, Pascal Roussel, Houria Kabbour

Unusual O^{2-}/F^{-} distribution in the new pyrochlore oxyfluorides: $Na_2B_2O_5F_2$ (*B*= Nb, Ta).

Edouard Boivin[a,*], Frédérique Pourpoint[a], Sébastien Saitzek[b], Pardis Simon[a], Pascal Roussel[a], Houria Kabbour[a,*]

a. *Univ. Lille, CNRS, Centrale Lille, ENSCL, Univ. Artois, UMR 8181-UCCS-Unité de Catalyse et Chimie du Solide, F-59000 Lille, France*
b. Univ. Artois, CNRS, Centrale Lille, Univ. Lille, UMR 8181, Unité de Catalyse et Chimie du Solide (UCCS), F-62300 Lens, France

edouard.boivin@univ-lille.fr ; houria.kabbour@univ-lille.fr

Abstract

Two new oxyfluorides with a pyrochlore-type structure, $Na_2Nb_2O_5F_2$ and $Na_2Ta_2O_5F_2$, have been obtained and for which the XRD crystallographic study coupled with ^{19}F solid state NMR reveals an unusual O/F distribution. Both materials are n-type semiconductors exhibiting photoconductive properties.

Among the well-known pyrochlore family, mixed anion phases offer great versatility and display a wide range of remarkable physical properties including cationic conductivity[1], ferroelectricity[2], magnetism[3] and photocatalytic activity[4]. Such properties may be tuned and potentially enhanced by the multiple anions interplay.[5] The pyrochlore $A_2B_2X_6X'$ structure is often described as two interconnected B_2X_6 and A_2X' sublattices with an anionic site X' (8b Wyckoff position of the Fd-3m space group, X'= O, N, F, S and/or vacancy (□)…) which possesses a great versatility towards mixed anions occupancy. On another hand, the X site (48d Wyckoff position, X= O, F or S) has almost always been reported as mono-anionic.[6] For instance, sulfur concentration in pyrochlore oxysulfides cannot exceed x=1 in $A_2B_2O_{7-x}S_x$ (*i.e.* $Cd_2Nb_2O_6S$ or $Sn_2Nb_2O_6S$)[7,8] due to the O/S size mismatch that drives the O/S ordering. In such case, the large 8b anionic site, located in the center of the pyrochlore channel, is ideal for a large anion such as S^{2-} contrarily to the 48f site. Similarly, in pyrochlore oxyfluorides, and although this size mismatch issue is limited, most of them do not exceed the x=1 fluorine content ($AA'B_2O_6F$, $(Li, La, □)_2B_2O_6F$ or Sn_2NbTiO_6F with A= alkali, A'= alkali earth, and B= Nb^{5+} and Ta^{5+})[1,8–10]. Therefore, fluorine is often located exclusively in the 8b site and hence the transition metal remains in an undistorted monoanionic BO_6 octahedra. So far, only a few pyrochlores-like compounds such as $Pb_2Ti_2O_{5.4}F_{1.2}$ provide a mixed anion environment for both A and B cation.[11] This compound possesses remarkable photocatalytic properties for overall water splitting under visible light irradiation thanks to distorted $Ti(O,F)_6$ octahedra and a large dielectric constant that drive the separation of the photogenerated electron/hole pairs.[4,11] This example

highlights the interest of exploring pyrochlore oxyfluorides with high F content, in order to impose the presence of fluorine in the transition metal coordination sphere as well as within the A_2X' framework and thus promote the photoconduction.

Submicrometric particles (diameter of 200-400 nm, see **Figure S1**) with approximate $Na_2B_2O_5F_2$ (B= Nb, Ta) composition have been obtained through a hydrothermal route from B_2O_5 (B =Nb, Ta) and NaF (as described in the experimental section in the SI). The solid state reaction between these precursors is known to produce $Na_2B_2O_5F_2$ composition but with a different structure.[12] On another hand the pyrochlore-like $NaTa_2O_5F$ phase is obtained by ion-exchange reaction from $RbTa_2O_5F$.[13] We thus present a direct and soft synthetic route which yield the new pyrochlores $Na_2B_2O_5F_2$. The elemental compositions have been obtained by a combination of EDX and XPS. Using both techniques, only Na, Nb, Ta, O, F and C spectral lines are observed (see **Figure S2**). The Na/Nb, F/Nb, Na/Ta and F/Ta atomic ratios extracted from XPS are 0.95 (0.97 from EDX), 1.0, 0.9 (0.93 from EDX) and 2.1 respectively (see **Table S1**) while the presence of C 1s core level is most probably related to the presence of a minor amount of surface organic contamination. A deficiency of Na compared with the $Na_2B_2O_5F_2$ composition is noticed. In order to clarify the origin of this slight off-stoichiometry, IR spectroscopy has been employed. A broad contribution centered around 3400cm^{-1} assigned to H-O stretching is accompanied to another at *ca.* 1630 cm^{-1} which is typical for H-O-H deformation within a water molecule and/or a hydronium cation. This is in good agreement with the loss of water observed by TGA-MS until *c.a.* 400°C (see **Figure S3**). Assuming Nb and Ta in their 5+ oxidation states and a M/F ratio close to 1 as both determined by XPS and the weight losses observed by TGA-MS, we estimate that the compositions of the materials are $Na_{1.9}(H_3O)_{0.1}Nb_2O_5F_2$ and $Na_{1.8}(H_3O)_{0.2}Ta_2O_5F_2$ (details are provided in the SI). Note that, the presence of H_3O^+ in A site of the pyrochlore structure has already been established in several compounds including Ta-based pyrochlores.[14] For sick of clarity, samples will be named as $Na_2B_2O_5F_2$ all along this article.

The Rietveld refinement of the structures in the *Fd*-3*m* space group is displayed in **Figure 1**. The refined cell parameters are 10.5181(3) Å and 10.5231(1) Å for the Nb and Ta based materials, respectively. However, especially for $Na_2Nb_2O_5F_2$, slight peak shifts with respect to the cubic lattice and selective broadening of the odd reflections of the Fd-3m space group could suggest the presence of anti-phase boundary defects (see **Figure S5**). A more detailed structural study of $Na_2Nb_2O_5F_2$ at the local scale would be necessary to verify this hypothesis. For the Rietveld refinements, the compositions have been fixed to that determined previously considering Na^+ in the 16c site (A site) together with a slight quantity of H_3O^+ as deduced from TGA. M is considered in a fully occupied 16d site (B site) and O and F statistically distributed in the 48f (X site) and 8b (X' site) sites of the *Fd*-3*m* space group. Moreover, the Rietveld quantification led to minor amounts of Nb_2O_5 (≈1 wt.%) or Ta_2O_5 (≈3 wt.%) impurities which were identified in the XRD patterns. The refined parameters and the agreement factors are summarized in the **Table S2.**

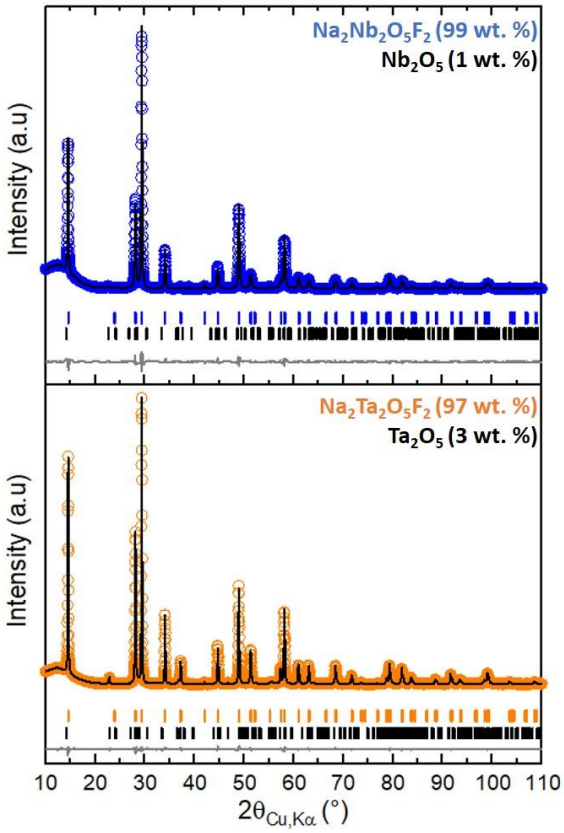

Figure 1: Rietveld refinement of the structure of $Na_2Nb_2O_5F_2$ (top panel) and $Na_2Ta_2O_5F_2$ (bottom panel) based on XRPD data.

Nb and Ta are in an octahedral site with Nb-X distances of 2.005(4) Å and Ta-X distances of 2.032(4) Å while Na occupies a site coordinated by 8 anions $NaX_6X'_2$ with Na-X = 2.644(9) Å and Na-X' = 2.277(2) Å in Nb-based material and Na-X = 2.597(9) Å and Na-X' = 2.278(2) Å in the Ta-based compound. The analysis of the BVS suggests a partial O/F ordering with the 8b anionic site of the *Fd*-3*m* space group fully occupied F^- and the 48f site statistically occupied by 83% of O^{2-} and 17% of F^- (see **Table S2**).

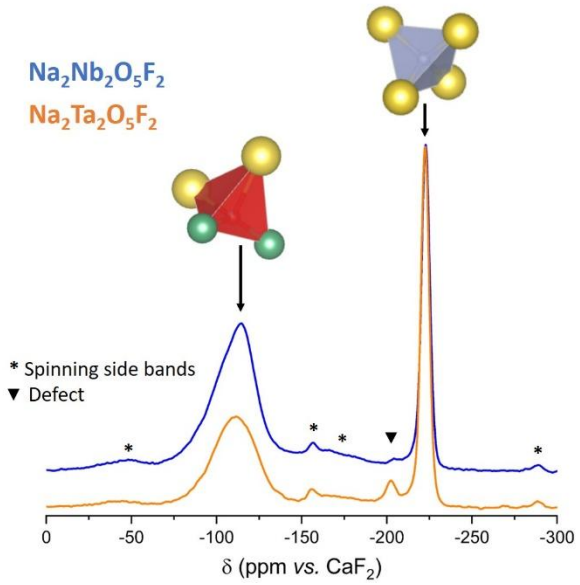

Figure 2: ^{19}F MAS NMR spectra of $Na_2Nb_2O_5F_2$ (blue) and $Na_2Ta_2O_5F_2$ (orange). The red and blue polyhedra represent the FNa_2B_2 *48d* site and the FNa_4 *8b* site, respectively.

In order to further support the unusual O/F distribution suggested by the BVS, ^{19}F MAS NMR has been employed for both compounds, see **Figure 2**. The spectra show two main contributions and a minor peak (which could arise from the presence of some H_3O^+ on the Na site). Both anionic sites of the pyrochlore structure are tetrahedrally coordinated, the 8b by four Na^+ and the 48f by two Na^+ and two M^{5+} (see **Figure 3**). Assuming some fluorine occupancy in the 8b position as suggested by the BVS analysis, the 48f position must contain some fluorine as well, in good agreement with NMR. The 8b site is in an undistorted and very ionic FNa_4 environment that could match with the sharp resonance at -222 ppm. Indeed, the calculation of the ^{19}F NMR shift thanks to the superposition model developed by Bureau et al.[15] for ionic fluorine predicts a shift of -238.3 ppm (for $Na_2Ta_2O_5F_2$) and -238.1 ppm (for $Na_2Nb_2O_5F_2$) vs. CaF_2 in rather good agreement with the experimental shift of -222 ppm but not with the broad peak centered around -110 ppm. Moreover, the experimental shift of the -222 ppm is rigorously equal for both phases. This agrees with the 8b site not localized in the neighboring of the transition metals hence preserving its local environment in both Nb and Ta phases. Stronger differences are observed between samples regarding the broad peak located at -110/-114 ppm which asymmetry suggests a strong dipolar interaction with the transition metal in good agreement with this NMR contribution being associated to fluorine localized in the 48f site. Moreover, the large line width indicates a wide chemical shift distribution produced by slightly different F-M bond lengths due to local distortions of the $B(O,F)_6$ octahedra averaged by XRD.

The full occupancy of the 8b site by F^- is very often observed in the oxyfluoride pyrochlores $A_2M_2O_6F$.[1,8–10] However, the presence of mixed O/F environments around the transition metals has been reported in only few pyrochlores-like materials such as $CsNb_2O_5F$, $CsMnMoO_3F_3$ and $Pb_2Ti_2O_{5.4}F_{1.2}$.[11,16,17] In $CsNb_2O_5F$ and $CsMnMoO_3F_3$ (S.G. = *Fd*-3*m*), the large Cs^+ ion can only be accommodated in the center of the pyrochlore channel (*i.e.* the 8b site, occupied by F^- in our materials) that forces the localization of the fluorine in the first coordination sphere of Nb (*i.e.* the 48f site) while the 16d site is empty. For $Pb_2Ti_2O_{5.4}F_{1.2}$ the distortion of Ti^{4+} octahedra allowed by the *F*-43*m* space group is driven by the partial O/F ordering which confers to TiO_3X_3 (X= 60% O, 40% F) octahedra a cis configuration.

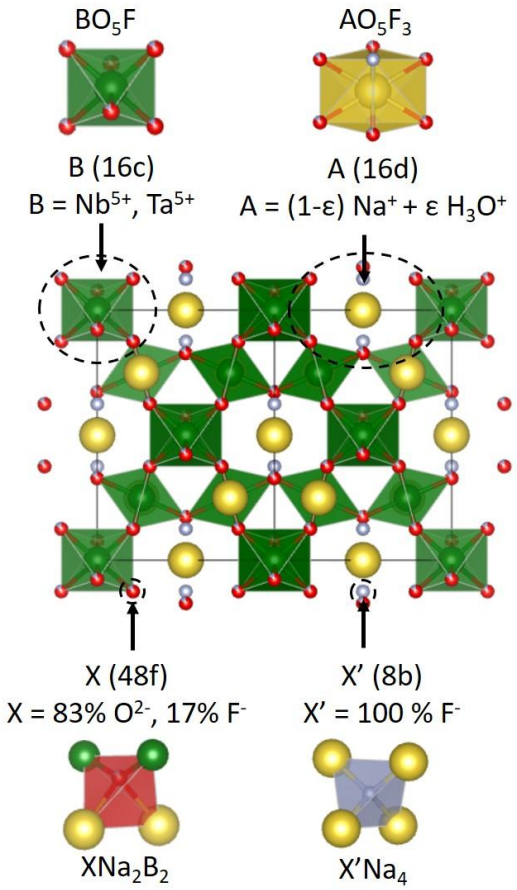

Figure 3: Structure of $Na_2B_2O_5F_2$ (B= Nb or Ta) with average environments of cations and anions as deduced from XRPD and ^{19}F MAS NMR. B is represented in green, Na in yellow, O in red and F in light blue.

The optical band gap of these two new pyrochlores oxyfluorides have been estimated by UV-Vis diffuse reflectance measurements. The Tauc plots (i.e. $(\alpha h\nu)n = f(h\nu)$, displayed in the **Figure 4a**) suggests an indirect band gap (n=2) of 3.65 and 3.75 eV for Nb and Ta-based oxyfluoride respectively, in good agreement with the white color of the samples and DFT calculation. Indeed, the calculated electronic structures on selected ordered models (**Figure 4b** and **Figure S6**) indicate similar topologies of the partial density of states (PDOS) for the Nb and Ta-phase. A higher indirect band gap is found for $Na_2Ta_2O_5F_2$ (3.36 eV for Nb and 3.74 eV for Ta) and all band gaps are in good agreement with experiment regarding the expected underestimation of the GGA method. Their PDOS reveal that, at the bottom of the conduction band, B site *nd* states are dominating and the top of the valence band is dominated by O 2*p* states, thus indicating a charge transfer insulator. On another hand, we can distinguish the contribution of fluorine in pure Na environment (FNa_4) which is as expected ionic. It shows a very localized contribution around -0.5 eV while the F 2*p* states of the fluorine atoms in FNa_2B_2 environments are rather delocalized in the same energy range than B states and mostly up to *c.a.* -2.0 eV. The Mott-Schottky plots of the both samples registered in the dark at 1 kHz are shown in the **Figure 4c**. These plots evidence linear domains with positive slopes typical for n-type semiconductors with a flat band potential of -1.18 V and -1.19 V vs. Ag/AgCl for $Na_2Nb_2O_5F_2$ and $Na_2Ta_2O_5F_2$ respectively. For n-type semiconductors, the flat band potential is localized at less than 0.1 V below the conduction band minimum (CBM).[18] Therefore, from the Mott-Schottky plot E_{CBM} ($Na_2Nb_2O_5F_2$) = -0.98 eV and E_{CBM} ($Na_2Ta_2O_5F_2$) = -0.99 eV vs. NHE, the corresponding valence

band maximum energy are E_{VBM} ($Na_2Nb_2O_5F_2$) = 2.67 eV and E_{VBM} ($Na_2Ta_2O_5F_2$) = 2.76 eV in very good agreement with that predicted from Mulliken electronegativity.[19] These band edge positions encompass the H^+/H_2, H_2O/O_2 redox voltages which make these materials potential candidates for overall water splitting photocatalysis. In order to further evaluate their potential, the photocurrent generation was investigated.

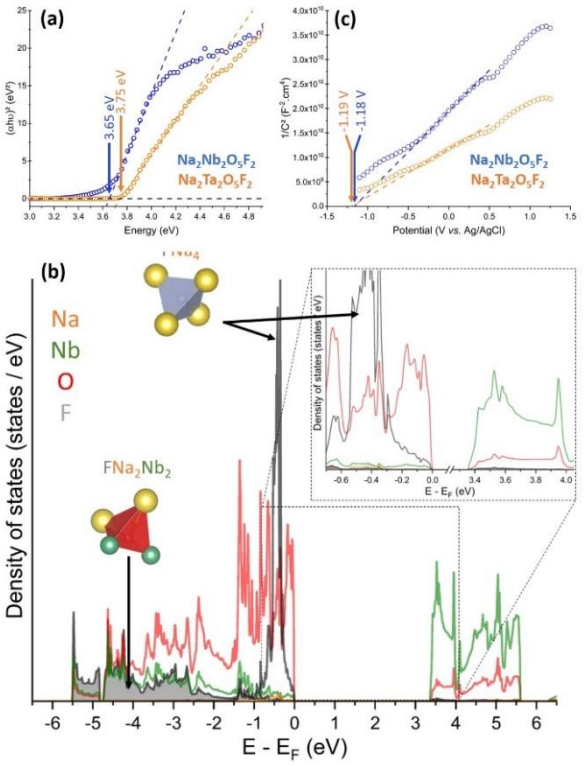

Figure 4: (a) The Tauc plot drawn from the UV-Visible diffuse reflectance spectra, (b) the PDOS of $Na_2Nb_2O_5F_2$. In inset the enlargement of the region nearby the Fermi (which is set to zero) and (c) Mott–Schottky plots

Figure 5a shows transient photocurrent response of $Na_2Nb_2O_5F_2$ as a function of the wavelength (from 450 nm to 655 nm) and measured at a bias voltage of 0.8 V *vs.* Ag/AgCl electrode. The variation of photocurrent density between dark and light clearly decreases when the wavelength increases until no significant current is detected from 590 nm. This shows that a small part of the visible light is well absorbed by the material to generate a photocurrent. The variation of the current density as a function of the light flux (ϕ) is represented in the **Figure 5b and 5c**. Overall, a nonlinear increase of the current density is observed with the flux. Indeed, the current density measured follows a $\Delta j=\alpha\phi^n$ law with n ≈ 0.71 and 0.59 for $Na_2Nb_2O_5F_2$ and $Na_2Ta_2O_5F_2$ respectively. This behavior can be assigned to the presence of structural defects acting as photo-electron traps within the structure.[20] Finally, the stable photocurrent upon successive measurements (**Fig. S7**) indicate very good stability of these samples.

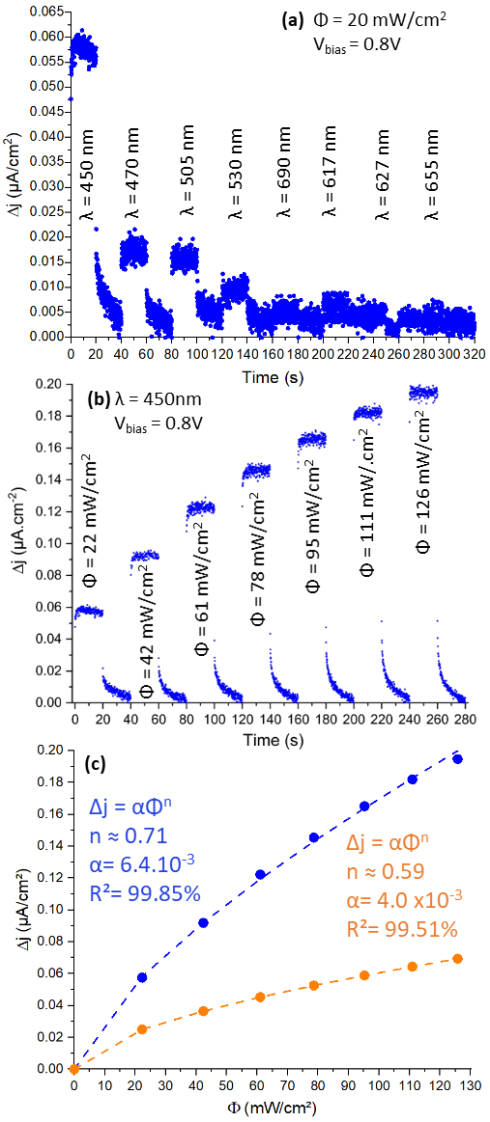

Figure 5: measurement of the current density of $Na_2Nb_2O_5F_2$ as a function of time for different (a) wavelengths (at constant flux of 20 mW/cm² and V_{Bias} = 0.8 V) and (b) flux (at constant wavelength of 450 nm and V_{Bias} = 0.8 V). (c) evolution of the current density as a function of the flux for both materials: $Na_2Nb_2O_5F_2$ (blue marks) and $Na_2Ta_2O_5F_2$ (orange marks).

In this article, through an accurate characterization of two new pyrochlore oxy-fluorides, $Na_2B_2O_5F_2$ (B= Nb, Ta), we highlight an unusual O/F distribution that implies mixed anion environments for both A and B cations. Photoconduction measurements on these wide band gap (>3.6 eV) n-type semiconductors reveal that they are photoactive and that their band edge positions are suitable for overall water splitting.

References

(1) Phraewphiphat, T.; Iqbal, M.; Suzuki, K.; Hirayama, M.; Kanno, R. *J. Japan Soc. Powder Powder Metall.* **2018**, *65* (1), 26–33.

(2) Bernard, D.; Le Montagner, S.; Pannetier, J.; Jacques, L. *Mater. Res. Bull.* **1971**, *6* (2), 75–80.

(3) Clark, L.; Nilsen, G. J.; Kermarrec, E.; Ehlers, G.; Knight, K. S.; Harrison, A.; Attfield, J. P.; Gaulin, B. D. *Phys. Rev. Lett.* **2014**, *113* (11), 7201.

(4) Kuriki, R.; Ichibha, T.; Hongo, K.; Lu, D.; Maezono, R.; Kageyama, H.; Ishitani, O.; Oka, K.; Maeda, K. *J. Am. Chem. Soc.* **2018**, *140* (21), 6648–6655.

(5) Kageyama, H.; Hayashi, K.; Maeda, K.; Attfield, J. P.; Hiroi, Z.; Rondinelli, J. M.; Poeppelmeier, K. R. *Nat. Commun.* **2018**, *9* (1), 772. Kabbour, H.; Sayede, A.; Saitzek, S.; Lefèvre, G.; Cario, L.;

Trentesaux, M.; Roussel, P. *Chemical Communications* **2020**, 56(11), 1645–1648
(6) Talanov, M. V.; Talanov, V. M. *Chem. Mater.* **2021**, *33*, 2706–2725.
(7) Laurita, G.; Hickox-Young, D.; Husremovic, S.; Li, J.; Sleight, A. W.; MacAluso, R.; Rondinelli, J. M.; Subramanian, M. A. *Chem. Mater.* **2019**, *31*, 7626–7637.
(8) Giampaoli, G.; Li, J.; Hermann, R. P.; Stalick, J. K.; Subramanian, M. A. *Solid State Sci.* **2018**, *81*, 32–42.
(9) Le Berre, F.; Crosnier-Lopez, M. P.; Galven, C.; Fourquet, J. L.; Legein, C.; Body, M.; Buzaré, J. Y. *Dalt. Trans.* **2007**, *23*, 2457–2466.
(10) Galven, C.; Legein, C.; Body, M.; Fourquet, J. L.; Buzarã, J. Y.; Le Berre, F.; Crosnier-Lopez, M. P. *Eur. J. Inorg. Chem.* **2010**, No. 33, 5272–5283.
(11) Oka, K.; Hojo, H.; Azuma, M.; Oh-Ishi, K. *Chem. Mater.* **2016**, *28* (15), 5554–5559.
(12) Vlasse, M.; Chaminade, J. P.; Massies, J. C.; Pouchard, M. *J. Solid State Chem.* **1975**, *12*, 102–109.
(13) Goodenough, J. B.; Hong, H. Y.; Kafalas, J. A. *Mater. Res. Bull.* **1976**, *11*, 203–220.
(14) Dickens, P. G.; Weller, M. T. *Solid State Commun.* **1986**, *59* (8), 569–573.
(15) Bureau, B.; Silly, G.; Buzaré, J. Y.; Emery, J. *Chem. Phys.* **1999**, *249*, 89–104.
(16) Fourquet, J.-L.; Jacoboni, C.; De Pape, R. *Mater. Res. Bull.* **1973**, *8*, 393–404.
(17) Atuchin, V. V; Molokeev, M. S.; Yurkin, G. Y.; Gavrilova, T. a; Kesler, V. G.; Laptash, N. M.; Flerov, I. N.; Patrin, G. S. *J. Phys. Chem. C* **2012**, *116*, 10162–10170.
(18) Kalanur, S. S. *Catalysts* **2019**, *9* (5).
(19) Butler, M. A.; Ginley, S. D. *J. Electrochem. Soc.* **1978**, *125* (2), 228–232.
(20) Ullrich, B.; Xi, H. Photocurrent Limit in Nanowires. *Opt. Lett.* **2013**, *38* (22), 4698.